Inorganic Chemistry

Article

pubs.acs.org/IC

Cd(II)-Coordination Framework: Synthesis, Anion-Induced Structural Transformation, Anion-Responsive Luminescence, and Anion Separation

Shan Hou, Qi-Kui Liu, Jian-Ping Ma, and Yu-Bin Dong*

College of Chemistry, Chemical Engineering and Materials Science, Key Laboratory of Molecular and Nano Probes, Engineering Research Center of Pesticide and Medicine Intermediate Clean Production, Ministry of Education, Shandong Provincial Key Laboratory of Clean Production of Fine Chemicals, Shandong Normal University, Jinan 250014, People's Republic of China

Supporting Information

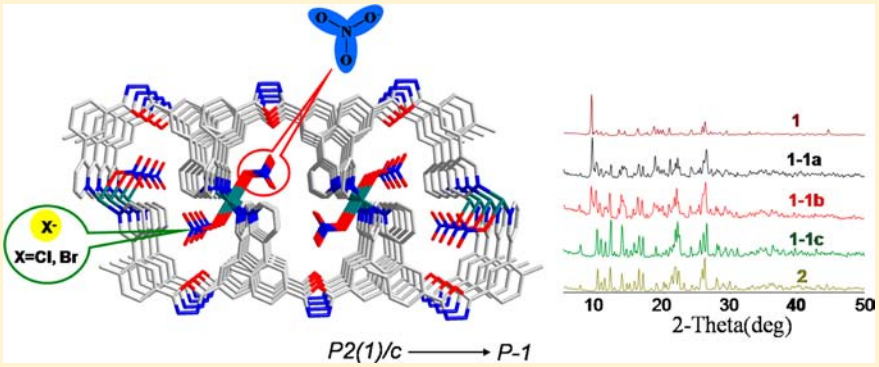

ABSTRACT: A series of Cd(II) coordination frameworks that are constructed from a new oxadiazole-bridged ligand 3,5-bis(3-pyridyl-3-(3′-methylphenyl)-1,3,4-oxadiazole (**L**) and CdX_2 (X = NO_3^-, Cl^-, Br^-, I^-, N_3^-, and SCN^-) were synthesized. The NO_3^- anion of the solid $CdL_2(NO_3)_2$·2THF (**1**) is able to be quantitatively exchanged with Cl^-, Br^-, I^-, SCN^-, and N_3^- in the solid state. For Cl^- and Br^-, the anion exchange resulted in a anion-induced structural transformation to form the structures of **2** and **3**, respectively. In addition, the Cd(II) structure herein exhibits the anion-responsive photoluminescence, which could be a useful method to monitor the anion-exchange process. Notably, compound **1** can recognize and completely separate SCN^-/N_3^- with similar geometry.

INTRODUCTION

As a new class of porous materials, polymeric coordination frameworks have great potential of being applied to adsorption, separation, luminescence, ion-exchange, catalysis, and sensor technology.[1] It is well-known that their structures could be controlled by ligand geometry and the metal center coordination mode. Very recently, the role of anions as templates for the construction of metal−organic frameworks (MOFs) and supramolecular assemblies has been receiving increasing attention.[2] To date, the anion template effect, however, has not been widely employed in determining the ultimate topology of MOFs. In most of the cases, MOF synthesis based on the anion template can be realized by changing counterions in the starting materials.[3] By contrast, the anion-exchange approach is considerably more challenging,[4] a fact that can be attributed to that the anion exchange would often result in the MOFs' disintegration when the anions diffuse in and out of the frameworks.

More importantly, anion exchange based on MOFs would result in the variation of optical and electrical parameters. Therefore, such a property has provided us a unique opportunity for construction of useful anion receptors, sensors, and separators.[5] On the other hand, anion exchange sometimes could cause the structural transformation; thus the anion exchange can be an additional approach for construction of new frameworks with different topological structures.

In this contribution, we report a series of interesting Cd(II) coordination frameworks based on a new oxadiazole-bridged ligand **L** and CdX_2 (X = NO_3^- (**1**), Cl^- (**2**), Br^- (**3**), I^- (**4**), N_3^- (**5**), and SCN^- (**6**)) salts. The NO_3^- anion of the solid $CdL_2(NO_3)_2$·2THF (**1**) is able to be quantitatively exchanged with Cl^-, Br^-, I^-, SCN^-, and N_3^- in the solid state. Some anion-exchange reactions, such as NO_3^- by Cl^- and Br^-, lead to anion-induced structural transformation. In addition, **1** herein exhibits the anion-responsive photoluminescence, which could be a useful method to monitor the anion-exchange process. Notably, compound **1** can recognize and completely separate SCN^-/N_3^- with similar geometry.

Received: December 10, 2012
Published: March 5, 2013

   dx.doi.org/10.1021/ic302716n | *Inorg. Chem.* 2013, 52, 3225−3235

Scheme 1. Synthesis of L and 1−6

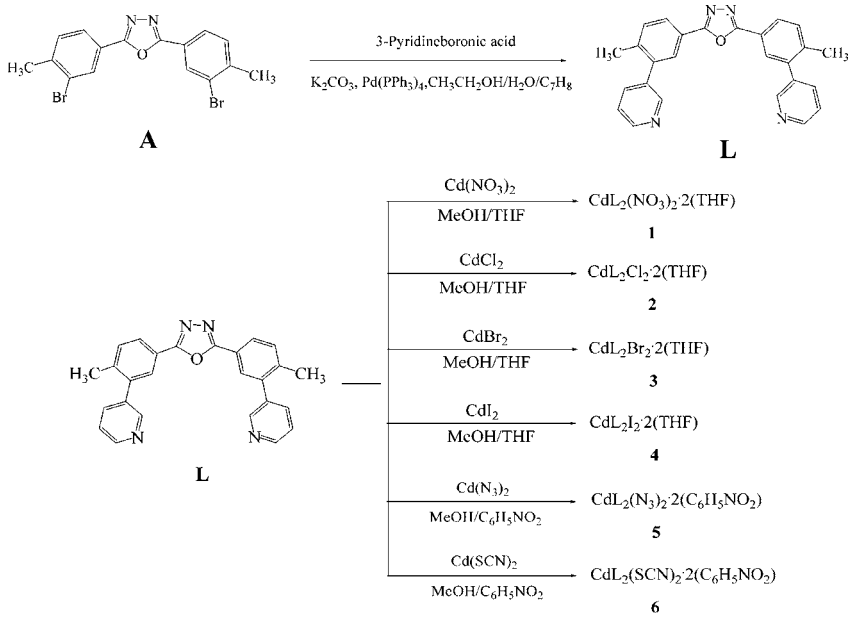

EXPERIMENTAL SECTION

Materials and Methods. Inorganic metal salts (Acros) were used as obtained without further purification. Infrared (IR) samples were prepared as KBr pellets, and spectra were obtained in the 400−4000 cm^{-1} range using a Perkin-Elmer 1600 FTIR spectrometer. Elemental analyses were performed on a Perkin-Elmer model 2400 analyzer. ^1H NMR data were collected using an AM-300 spectrometer. Chemical shifts are reported in δ relative to TMS. All fluorescence measurements were carried out on a Cary Eclipse Spectrofluorimeter (Varian, Australia) equipped with a xenon lamp and quartz carrier at room temperature. Thermogravimetric analyses were carried out using a TA Instrument SDT 2960 simultaneous DTA-TGA under flowing nitrogen at a heating rate of 10 °C/min. XRD patterns were obtained on a D8 ADVANCE X-ray powder diffractometer (XRD) with Cu Kα radiation (λ = 1.5405 Å). ICP-LC was performed on an IRIS Interpid II XSP and NU AttoM.

Synthesis of L. A mixture of 3,5-bis(3-bromo-4-methylphenyl)-1,3,4-oxadiazole (**A**: 4.08 g, 10.0 mmol) and 3-pyridineboronic acid (2.95 g, 24 mmol), $Pd(PPh_3)_4$ (1.16 g, 1.0 mmol), and K_2CO_3 (4.15 g, 30.0 mmol) in a EtOH/H_2O/toluene system was refluxed for 48 h. After removal of the solvent under vacuum, the residue was purified on silica gel by a column using CH_2Cl_2/THF = 4:1 as the eluent to afford **L** as a colorless crystalline solid (3.10 g; yield, 74%). IR (KBr pellet cm^{-1}): 3041(w), 1616(ms), 1589(s), 1499(s), 1385(vs), 1238(s), 1073(ms), 898 (ms), 810(s), 734(vs), 719(s). ^1H NMR (300 MHz, $CDCl_3$, 25 °C, TMS, ppm): 8.64−8.65 (t, 2H, $-C_5H_4N$), 8.08−8.10 (d, 1H, $-C_6H_3$), 7.98 (s, 1H, $-C_6H_3$), 7.72−7.74 (d, 1H, $-C_6H_3$), 7.46−7.49 (d, 1H, $-C_5H_4N$), 7.42−7.45 (t, 1H, $-C_6H_3$), 2.36 (s, 3H, $-CH_3$). Elemental analysis (%) calcd for $C_{26}H_{20}N_4O$: C, 77.21; H, 4.98; N, 13.85. Found: C, 77.53; H, 4.87; N, 14.21.

Synthesis of 1 ($CdL_2(NO_3)_2$·2THF). A solution of $Cd(NO_3)_2$ (6.0 mg, 0.020 mmol) in MeOH (7 mL) was carefully layered onto a solution of **L** (8.1 mg, 0.020 mmol) in THF (8 mL). The solutions were left for about 3 days at room temperature, and colorless crystals of **1** were obtained. Yield, 69%. IR (KBr pellet cm^{-1}): 2977(w), 1616(ms), 1555(s), 1434(s), 1384(vs), 1292(vs), 1031(ms), 904(s), 818(s), 737(s), 714(s). ^1H NMR (300 MHz, DMSO, 25 °C, TMS, ppm): 8.63−8.65 (t, 4H, $-C_5H_4N$), 8.09−8.11 (d, 2H, $-C_6H_3$), 7.99 (s, 2H, $-C_6H_3$), 7.88−7.90 (d, 2H, $-C_6H_3$), 7.57−7.60 (d, 2H, $-C_5H_4N$), 7.50−7.54 (t, 2H, $-C_6H_3$), 3.58−3.60 (t, 4H, C_4H_8O), 2.31 (s, 6H, $-CH_3$), 1.74−1.76 (t, 4H, C_4H_8O). Elemental analysis (%) calcd for $C_{60}H_{56}CdN_{10}O_{10}$: C, 60.58; H, 4.75; N, 11.75. Found: C, 60.94; H, 4.79; N, 11.91.

Synthesis of 2 (CdL_2Cl_2·THF). A solution of $CdCl_2$ (4.8 mg, 0.020 mmol) in MeOH (7 mL) was carefully layered onto a solution of **L** (8.1 mg, 0.020 mmol) in THF (8 mL). The solutions were left for about 5 days at room temperature, and colorless crystals of **2** were obtained. Yield, 41%. IR (KBr pellet cm^{-1}): 2974(w), 1616(ms), 1550(s), 1495(vs), 1417(vs), 1195(s), 1036(ms), 900(s), 815(s), 735(s), 712(vs). ^1H NMR (300 MHz, DMSO, 25 °C, TMS, ppm): 8.64−8.66 (t, 4H, $-C_5H_4N$), 8.10−8.13 (d, 2H, $-C_6H_3$), 8.01 (s, 2H, $-C_6H_3$), 7.89−7.91 (d, 2H, $-C_6H_3$), 7.58−7.61 (d, 2H, $-C_5H_4N$), 7.50−7.54 (t, 2H, $-C_6H_3$), 3.59−3.61 (t, 4H, C_4H_8O), 2.32 (s, 6H, $-CH_3$), 1.74−1.76 (t, 4H, C_4H_8O). Elemental analysis (%) calcd for $C_{56}H_{48}CdCl_2N_8O_3$: C, 63.19; H, 4.55; N, 10.53. Found: C, 63.62; H, 4.66; N, 10.77.

Synthesis of 3 (CdL_2Br_2·THF). A solution of $CdBr_2$ (6.8 mg, 0.020 mmol) in MeOH (7 mL) was carefully layered onto a solution of **L** (8.1 mg, 0.020 mmol) in THF (8 mL). The solutions were left for about 5 days at room temperature, and colorless crystals of **3** were obtained. Yield, 54%. IR (KBr pellet cm^{-1}): 2972(w), 1616(ms), 1550(s), 1469(vs), 1389(vs), 1195(s), 1036(ms), 943(s), 813(s), 711(s), 660(s). ^1H NMR (300 MHz, DMSO, 25 °C, TMS, ppm): 8.62−8.64 (t, 4H, $-C_5H_4N$), 8.09−8.12 (d, 2H, $-C_6H_3$), 8.00 (s, 2H, $-C_6H_3$), 7.89−7.91 (d, 2H, $-C_6H_3$), 7.57−7.60 (d, 2H, $-C_5H_4N$), 7.51−7.55 (t, 2H, $-C_6H_3$), 3.58−3.60 (t, 4H, C_4H_8O), 2.31 (s, 6H, $-CH_3$), 1.74−1.76 (t, 4H, C_4H_8O). Elemental analysis (%) calcd for $C_{56}H_{48}CdBr_2N_8O_3$: C, 58.32; H, 4.20; N, 9.72. Found: C, 57.86; H, 4.26; N, 9.69.

Synthesis of 4 (CdL_2I_2·THF). A solution of CdI_2 (7.2 mg, 0.020 mmol) in MeOH (7 mL) was carefully layered onto a solution of **L** (8.1 mg, 0.020 mmol) in THF (8 mL). The solutions were left for about 3 days at room temperature, and colorless crystals of **4** were obtained. Yield, 71%. IR (KBr pellet cm^{-1}): 2970(w), 1615(ms), 1547(s), 1470(vs), 1386(s), 1192(s), 1063(ms), 835(s), 818(s), 736(s), 712(s). ^1H NMR (300 MHz, DMSO, 25 °C, TMS, ppm): 8.62−8.64 (t, 4H, $-C_5H_4N$), 8.09−8.11 (t, 2H, $-C_6H_3$), 7.99 (s, 2H, $-C_6H_3$), 7.88−7.90 (d, 2H, $-C_6H_3$), 7.57−7.60 (d, 2H, $-C_5H_4N$), 7.50−7.53 (t, 2H, $-C_6H_3$), 3.58−3.60 (t, 4H, C_4H_8O), 2.31 (s, 6H, $-CH_3$), 1.74−1.76 (t, 4H, C_4H_8O). Elemental analysis (%) calcd for $C_{60}H_{56}CdI_2N_8O_4$: C, 54.62; H, 4.28; N, 8.49. Found: C, 54.97; H, 4.43; N, 8.63.

Synthesis of 5 ($CdL_2(N_3)_2$·2($C_6H_5NO_2$)). A solution of $Cd(N_3)_2$ (6.0 mg, 0.020 mmol) in MeOH (7 mL) was carefully layered onto a solution of **L** (8.1 mg, 0.020 mmol) in nitrobenzene (8 mL). The solutions were left for about a week at room temperature, and colorless crystals of **5** were obtained. Yield, 45%. IR (KBr pellet cm^{-1}):

dx.doi.org/10.1021/ic302716n | Inorg. Chem. 2013, 52, 3225−3235

Table 1. Synthesis of 1−6 and Their Space Groups

	$Cd(NO_3)_2$	$CdCl_2$	$CdBr_2$	CdI_2	$Cd(N_3)_2$	$Cd(SCN)_2$
L	**1**	**2**	**3**	**4**	**5**	**6**
solvent	MeOH/THF	MeOH/THF	MeOH/THF	MeOH/THF	MeOH/nitrobenzene	MeOH/nitrobenzene
space group	$P2(1)/c$	$P\bar{1}$	$P\bar{1}$	$P\bar{1}$	$P\bar{1}$	$P\bar{1}$

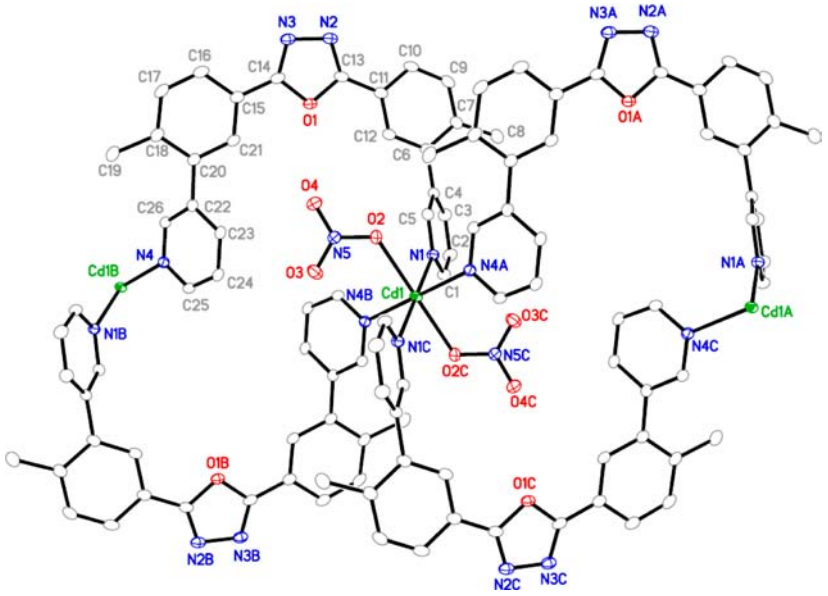

Figure 1. ORTEP figure of **1** showing four ligands surrounding one Cd(II) octahedral (30% ellipsoids).

2973(w), 2034(vs), 1616(ms), 1553(s), 1474(s), 1391(s), 1273(ms), 1192(s), 1064(s), 816(ms), 737(s), 714(s). ^{1}H NMR (300 MHz, DMSO, 25 °C, TMS, ppm): 8.62−8.64 (t, 4H, $-C_5H_4N$), 8.25−8.22 (d, 2H, $C_6H_5NO_2$), 8.09−8.11 (d, 2H, $-C_6H_3$), 7.99 (s, 2H, $-C_6H_3$), 7.88−7.90 (d, 2H, $-C_6H_3$), 7.82 −7.84 (d, 1H, $C_6H_5NO_2$), 7.65 −7.70 (t, 2H, $C_6H_5NO_2$), 7.57−7.61 (d, 2H, $-C_5H_4N$), 7.50−7.54 (t, 2H, $-C_6H_3$), 2.31 (s, 6H, $-CH_3$). Elemental analysis (%) calcd for $C_{64}H_{50}CdN_{16}O_4$: C, 61.42; H, 4.03; N, 17.91. Found: C, 61.74; H, 4.15; N, 18.05.

Synthesis of 6 ($CdL_2(SCN)_2$·2($C_6H_5NO_2$)). A solution of $Cd(SCN)_2$ (4.8 mg, 0.020 mmol) in MeOH (7 mL) was carefully layered onto a solution of **L** (8.1 mg, 0.020 mmol) in nitrobenzene (8 mL). The solutions were left for about a week at room temperature, and colorless crystals of **6** were obtained. Yield, 42%. IR (KBr pellet cm^{-1}): 2856(w), 2045(vs), 1616(ms), 1578(ms), 1475(s), 1399(s), 1193(ms), 1033(ms), 838(ms), 736(s), 714(s). ^{1}H NMR (300 MHz, DMSO, 25 °C, TMS, ppm): 8.62−8.65 (t, 4H, $-C_5H_4N$), 8.25−8.22 (d, 1H, $C_6H_5NO_2$), 8.11−8.13 (d, 2H, $-C_6H_3$), 7.91 (s, 2H, $-C_6H_3$), 7.89−7.91 (d, 2H, $-C_6H_3$), 7.82−7.84 (d, 1H, $C_6H_5NO_2$), 7.68−7.71 (t, 2H, $C_6H_5NO_2$), 7.58−7.61 (d, 2H, $-C_5H_4N$), 7.53−7.55 (t, 2H, $-C_6H_3$), 2.32 (s, 6H, $-CH_3$). Elemental analysis (%) calcd for $C_{66}H_{50}CdN_{12}O_6S_2$: C, 61.75; H, 3.93; N, 13.09; S, 5.00. Found: C, 62.23; H, 4.07; N, 12.96; S, 5.12.

Single-Crystal Analysis. For **1−6**, X-ray intensity data were measured on a Bruker SMART APEX CCD-based diffractometer (Mo Kα radiation, λ = 0.71073 Å). The raw frame data were integrated into SHELX-format reflection files and corrected for Lorentz and polarization effects using SAINT.[6] Corrections for incident and diffracted beam absorption effects were applied using SADABS.[6] None of the crystals showed evidence of crystal decay during data collection. All structures were solved by a combination of direct methods and difference Fourier syntheses and refined against F^2 by the full-matrix least-squares technique. Crystal data, data collection parameters, and refinement statistics are listed in Tables 2 and 3.

RESULTS AND DISCUSSION

Synthesis. Ligand 3,5-bis(3-pyridyl-3-(3′-methylphenyl)-1,3,4-oxadiazole (**L**) was prepared by the combination of 3,5-bis(3-bromo-4-methylphenyl)-1,3,4-oxadiazole and 3-pyridineboronic acid by Pd-catalyzed Suzuki coupling reaction in good yield. As shown in Scheme 1, **L** is a symmetric ligand that contains two rigid methyl-substituted 3-pyridylphenyl arms. The introduced methyl groups effectively enhance the ligand solubility in organic solvents, which facilitates the reactions between it and metal ions in solutions. As shown in Table 1, compounds **1−6** were prepared by the combination of CdX_2 (X = NO_3^-, Cl^-, Br^-, I^-, N_3^-, and SCN^-) and **L** in the mixed solvent systems in moderate yields. These crystalline solids are stable in air and insoluble in common organic solvents and water due to their polymeric nature.

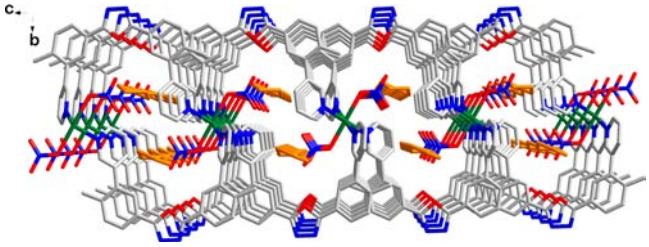

Figure 2. Crystal packing showing the THF guest molecules and NO_3^- anions located in the distorted ellipse-like channels. THF molecule is highlighted in orange for clarity.

Crystal Structure Descriptions. *Crystal Structure of 1.* Compound **1** ($Cd(L)_2(NO_3)_2$·2(THF)) is well demonstrated by X-ray single-crystal analysis. As shown in Figure 1, each Cd(II) center adopts a distorted octahedral $\{CdN_4O_2\}$

dx.doi.org/10.1021/ic302716n | Inorg. Chem. 2013, 52, 3225−3235

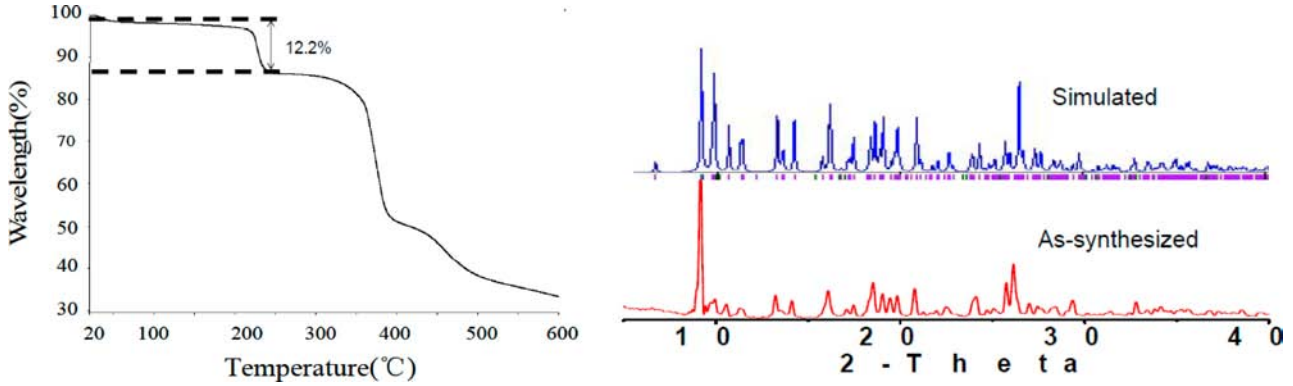

Figure 3. TGA trace (left) and XRPD patterns (right) of **1**.

Table 2. Crystal Data and Structure Refinement for 1−3

compound	1	2	3
empirical formula	$C_{60}H_{56}CdN_{10}O_{10}$	$C_{56}H_{48}CdCl_2N_8O_3$	$C_{56}H_{48}CdBr_2N_8O_3$
formula weight	1189.55	1064.32	1153.24
temp (K)	123(2)	123(2)	123(2)
crystal system	monoclinic	triclinic	triclinic
space group	$P2(1)/c$	$P\bar{1}$	$P\bar{1}$
a (Å)	10.5162(11)	8.805(2)	8.878(4)
b (Å)	26.572(3)	11.243(3)	11.332(5)
c (Å)	10.3753(11)	12.730(3)	12.743(5)
α (deg)	90	77.884(4)	78.186(6)
β (deg)	113.3420(10)	73.974(4)	73.722(6)
γ (deg)	90	82.865(3)	83.114(6)
V (Å^3)	2662.0(5)	1181.2(5)	1201.9(8)
Z	2	1	1
ρcalc (g/cm^3)	1.484	1.496	1.593
F(000)	1228	546	582
data/restraints/params	5007/0/369	4361/5/312	4391/5/330
GOF on F^2	1.055	1.034	1.035
final R indices [$I > 2\sigma(I)$]	R1 = 0.0363	R1 = 0.0447	R1 = 0.0645
	wR2 = 0.0885	wR2 = 0.0986	wR2 = 0.1530

Table 3. Crystal Data and Structure Refinement for 4−6

compound	4	5	6
empirical formula	$C_{60}H_{56}CdI_2N_8O_4$	$C_{64}H_{50}CdN_{16}O_6$	$C_{66}H_{50}CdN_{12}O_6S_2$
formula weight	1319.33	1251.60	1283.70
temp (K)	123(2)	123(2)	298(2)
crystal system	triclinic	triclinic	triclinic
space group	$P\bar{1}$	$P\bar{1}$	$P\bar{1}$
a (Å)	9.9786(15)	9.5361(19)	9.456(3)
b (Å)	11.4301(18)	11.028(2)	11.302(4)
c (Å)	12.1622(19)	13.700(3)	14.170(5)
α (deg)	95.781(2)	78.409(3)	77.928(5)
β (deg)	102.037(2)	84.306(3)	82.782(6)
γ (deg)	95.162(2)	84.036(3)	84.890(6)
V (Å^3)	1341.0(4)	1399.2(5)	1466.0(8)
Z	1	1	1
ρcalc (g/cm^3)	1.634	1.485	1.454
F(000)	658	642	658
data/restraints/params	4924/0/342	5155/0/396	5400/0/396
GOF on F^2	1.034	1.050	1.023
final R indices [$I > 2\sigma(I)$]	R1 = 0.0377	R1 = 0.0507	R1 = 0.0688
	wR2 = 0.0959	wR2 = 0.1055	wR2 = 0.1261

environment involving four N atoms from four **L** ligands and two O atoms from two monodentate nitrate. The Cd−N bond lengths are 2.347(2) and 2.3538(19) Å,[7] respectively, while the axial Cd−O distance is 2.3563(18) Å.[8] The Cd(II) nodes are

dx.doi.org/10.1021/ic302716n | *Inorg. Chem.* 2013, 52, 3225−3235

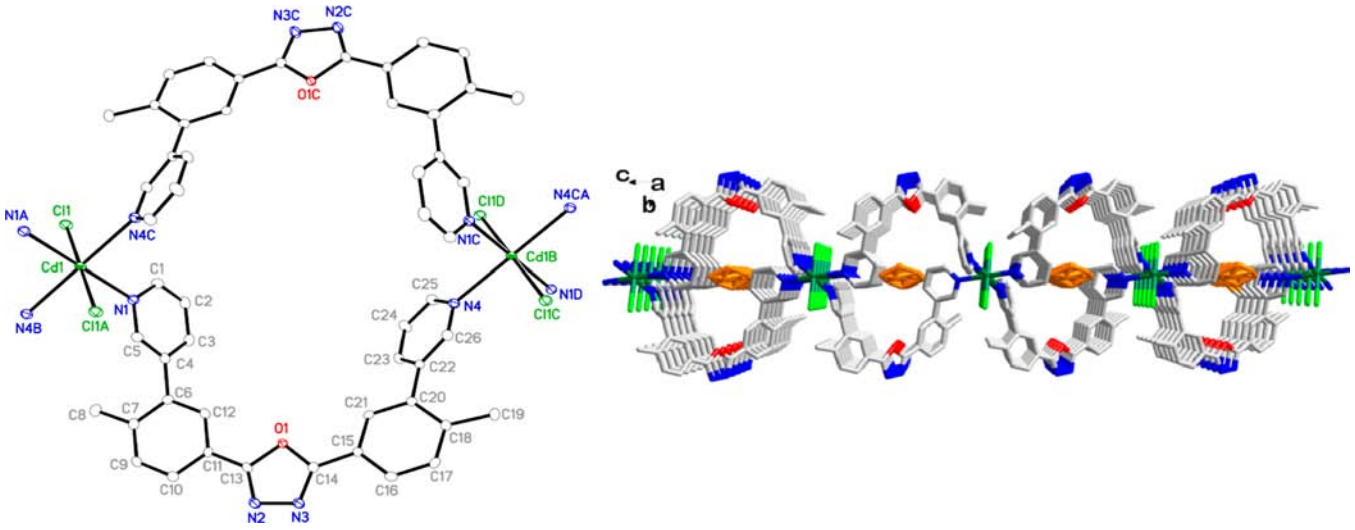

Figure 4. Left: ORTEP figure of **2** showing four ligands surrounding one Cd(II) octahedral (30% ellipsoids). Right: Crystal packing of **2** showing the THF guest molecules located in the distorted ellipse-like channels. THF molecule is highlighted for clarity.

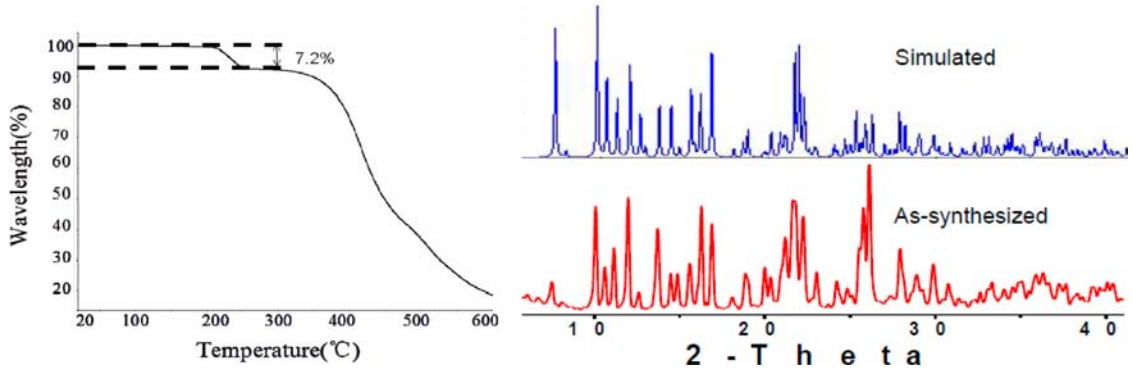

Figure 5. Left: TGA trace of **2**. The calculated and observed weight losses corresponding to encapsulated THF are 6.77 and 7.2%, respectively. Right: XRPD patterns (right) of **2**.

Scheme 2. Anion Exchange Based on 1

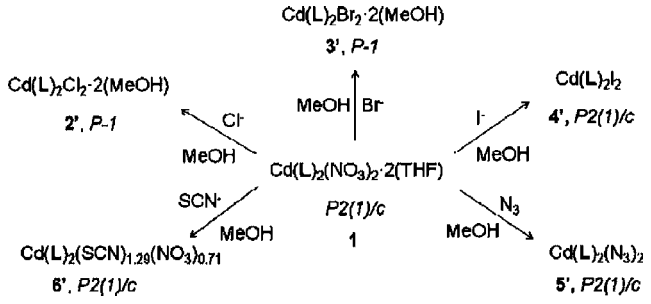

connected to each other to form an infinite 1D chain that consists of a 34-membered bimetallic macrocycle-containing building block, in which the two terminal pyridyl groups on each *cis*-**L** ligand are basically perpendicular to each other. In each elliptical ring, the Cd(II)···Cd(II) contact is around 10 Å, while the opposite oxadiazole O···O distance is around 12 Å. These 1D macrocycle-containing chains (Supporting Information) stack together in -AA- fashion along the crystallographic *a* axis to generate distorted ellipse-like channels, in which the coordinated NO_3^- anions and THF guest molecules are located (Figure 2), which is further confirmed by thermogravimetric analysis (Figure 3). Thermogravimetric analysis (TGA, Figure 3) revealed that the encapsulated THF could be completely removed at temperatures ranging from 200 to 230 °C (calculated 12.1%, observed 12.2%). The XRPD patterns based on the desolvated sample of **1** confirms that the **CdL**$_2$ framework is stable.

Crystal Structures of 2–6. To confirm the templating effect of different anions in the self-assembly process, spherical halide anions Cl^-, Br^-, and I^- and linear triatomic N_3^- and SCN^- were used instead of triangular NO_3^- to perform the reactions. Single-crystal analysis revealed that compounds **2–6** are isostructural. They all crystallize in the triclinic space group $P\bar{1}$ (Supporting Information and Tables 2 and 3), which is different from that of **1**. Therefore, only the structure of **2** is described in detail herein. The resolved solid-state structure indicated that each Cd(II) node has a coordination environment around the Cd(II) ion similar to that of **1**, but the axial positions of the octahedron in **2** are occupied by two Cl^- anions. It is different from **1**; the terminal pyridyl sites on each *cis*-**L** ligand face to opposite directions and bind two Cd(II) ions into a relative regular elliptical ring with a Cd(II)···Cd(II) distance of ca. 13 Å. It is similar to **1**; **2** also features the bimetallic elliptical ring-containing 1D chain motif (Supporting Information). Furthermore, the 1D chain stacks upon its neighbors along the crystallographic *a* axis to generate large ellipse-like channels that encapsulate the disordered THF molecules (Figure 4). The TGA trace indicated that the

dx.doi.org/10.1021/ic302716n | *Inorg. Chem.* 2013, 52, 3225–3235

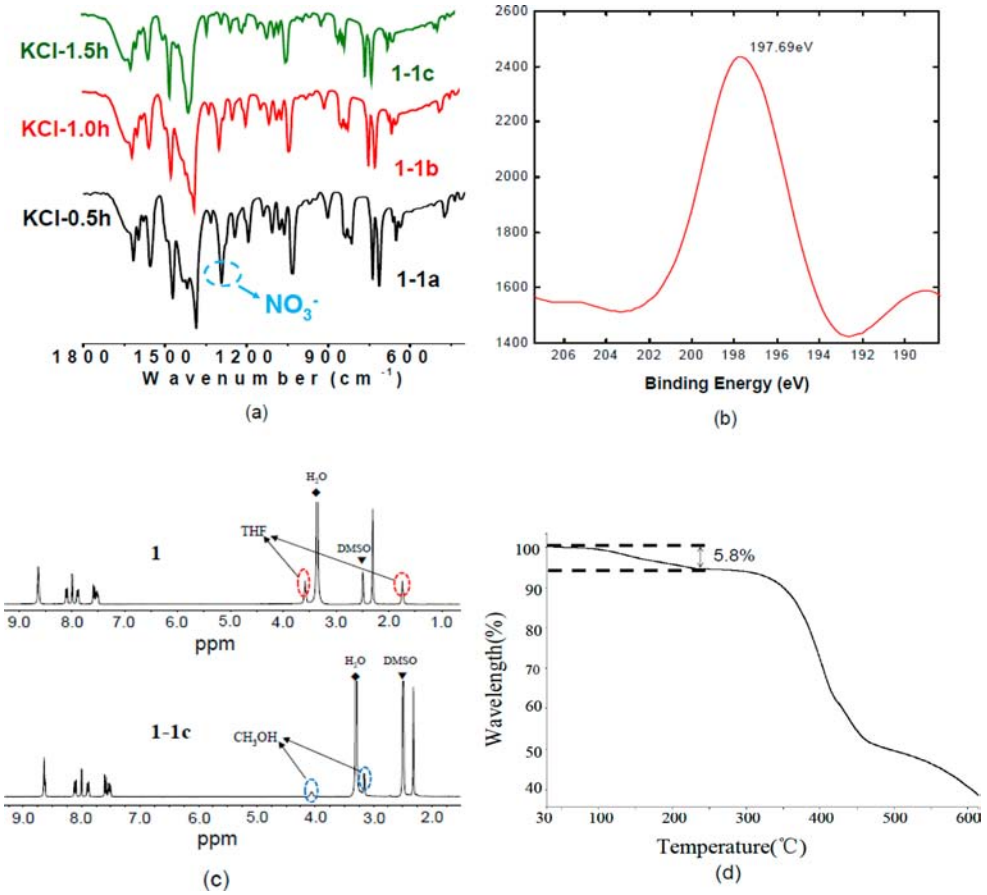

Figure 6. (a) IR spectra monitoring of **1**, **1-1a** (0.5 h), **1-1b** (1.0 h), and **1-1c** (1.5 h). (b) XPS spectrum of **1-1c**. (c) ^{1}H NMR spectrum of **1** and **1-1c**. (d) TGA trace of **1-1c**. The calculated MeOH amount depending on $CdL_2Cl_2 \cdot 3MeOH$ is 5.9%, and the observed amount is 5.8%.

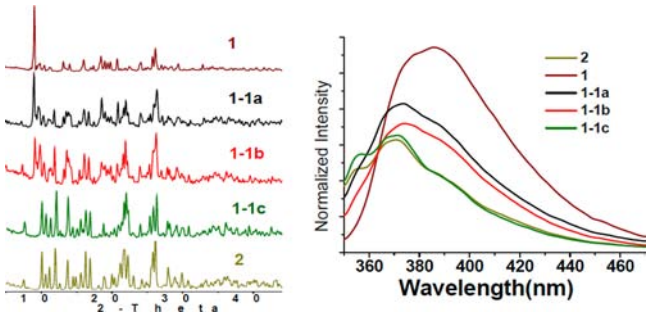

Figure 7. Left: XRPD patterns of **1**, **1-1a** (0.5 h), **1-1b** (1.0 h), **1-1c** (1.5 h), and **2**. Right: Solid-state luminescent spectra of **1**, **1-1a** (0.5 h), **1-1b** (1.0 h), **1-1c** (1.5 h), and **2** upon excitation at 343 nm.

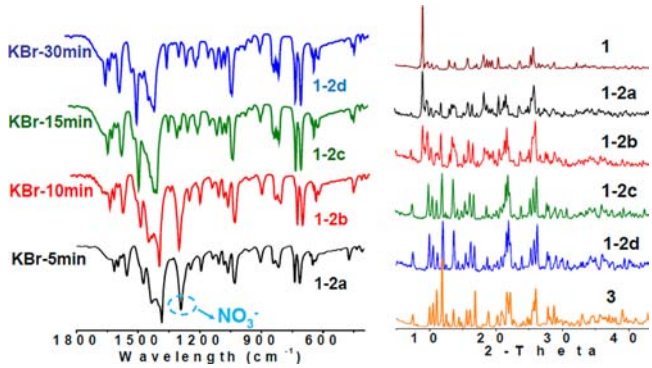

Figure 8. Left: IR spectra monitoring of **1**, **1-2a** (5 min), **1-2b** (10 min), **1-2c** (15 min), and **1-2d** (30 min). Right: XRPD patterns of **1**, **1-2a** (5 min), **1-2b** (10 min), **1-2c** (15 min), **1-2d** (30 min), and **3**.

encapsulated THF molecules can be removed by heating from 200 to 250 °C (Figure 5). The remarkable difference between **1** and **2** lies in the location of the anions. As mentioned above, the NO_3^- anion in **1** faces toward the center of the channel, whereas the Cl^- anion in **2** is vertical to the ring plane and located between the channels. Again, the XRPD pattern indicated that the as-synthesized compound **2** is pure (Figure 5).

Anion Exchange Based on 1. Besides the functions of binding metal node, charge balance, and so on, the anion species sometimes might induce the structural transformation by anion exchange.[4a,9] As demonstrated by the crystal structure of **1**, the counteranions are located in the channels of the structures (Figure 2). In addition, compound **1** is insoluble in common organic solvents; therefore, it is expected to display anion-exchange properties in the solid state (see Scheme 2).

After a suspension of the crystals of **1** in a saturated MeOH solution of KCl at room temperature, the solid was isolated by filtration, washed with MeOH several times, and dried in air. The IR spectra[10] monitoring shows that the strong band associated with NO_3^- at 1292(vs) cm^{-1} is significantly weakened as time goes on, indicating that the NO_3^- in **1** was exchanged by the incursive Cl^- (Figure 6a). After 1.5 h, the NO_3^- was completely replaced by Cl^- depending on the IR spectrum to generate CdL_2Cl_2 (**1-1c**). Besides the IR monitoring, the anion exchange is also confirmed by X-ray

dx.doi.org/10.1021/ic302716n | Inorg. Chem. 2013, 52, 3225−3235

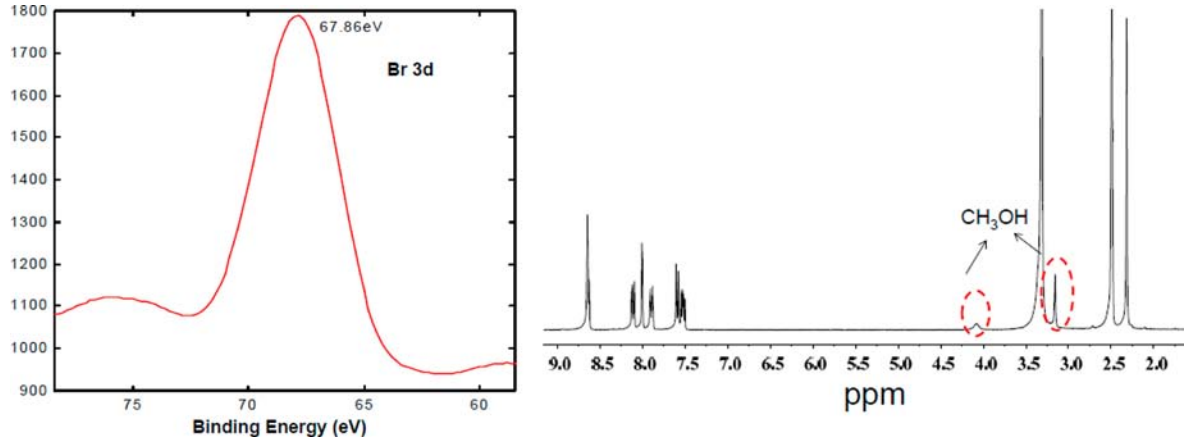

Figure 9. Left: XPS spectrum of **1-2d**. Right: ^{1}H NMR spectrum of **1-2d**.

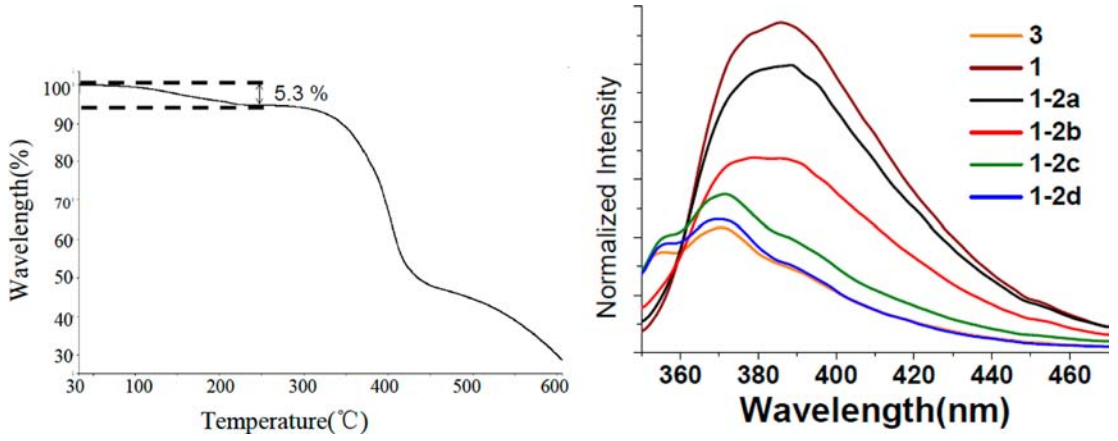

Figure 10. Left: TGA trace of **1-2d** (observed and calculated MeOH weight losses are 5.6 and 5.3%, respectively). Right: Solid-state luminescent spectra (λ_{ex} = 343 nm) of **1**, **1-2a**, **1-2b**, **1-2c**, **1-2d**, and **3**.

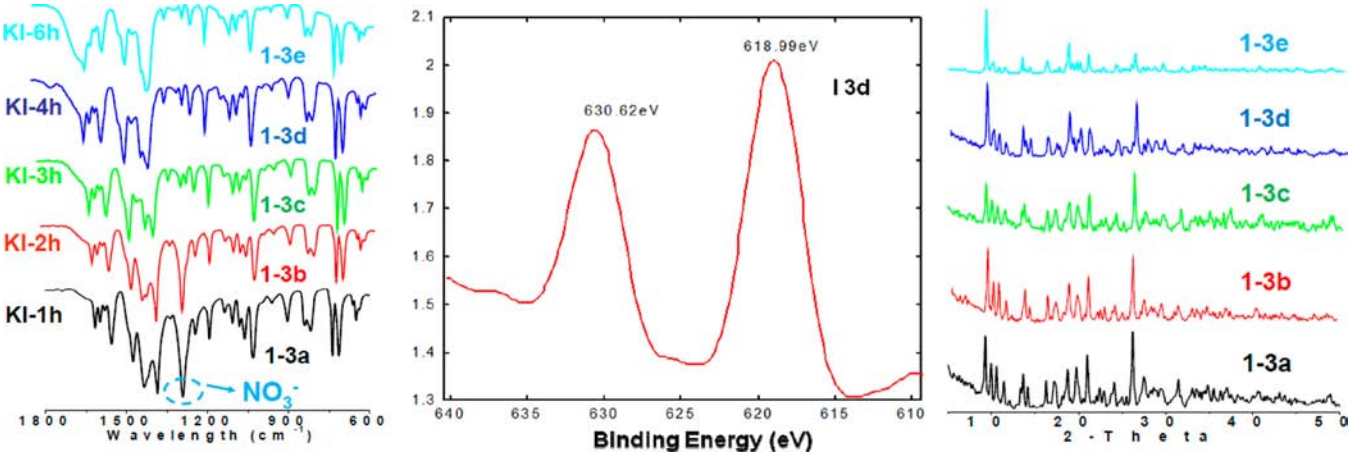

Figure 11. Left: IR spectra of **1** stirred in a MeOH solution of KI at 1−6 h, respectively. Middle: XPS spectrum of **1-3e**. Right: Corresponding XRPD patterns of **1-3a** to **1-3e**.

photoelectron spectroscopy (XPS) measurement. As shown in Figure 6b, XPS observation of the Cl 2p (197.69 eV) peak well supports that the anion-exchange reaction occurred and the existence of chlorine. On the other hand, the ^{1}H NMR spectrum (Figure 6c), together with the TGA measurement (Figure 6d), on the exchanged sample demonstrates that the encapsulated THF molecules are simultaneously replaced by the MeOH molecules when the reaction was carried out in the MeOH medium. The ion chromatograph (For $CdL_2Cl_2{\cdot}3CH_3OH$, the calculated and observed Cl^- amounts are 6.51 and 6.06%, respectively) indicated that the NO_3^- in **1** was almost quantitatively exchanged with Cl^-.

Interestingly, the XRPD pattern monitoring indicates that an anion-induced structural transformation occurred during the anion exchange. As shown in Figure 7, the peaks corresponding to **2** gradually appeared while the peaks of **1** disappeared by

dx.doi.org/10.1021/ic302716n | Inorg. Chem. 2013, 52, 3225−3235

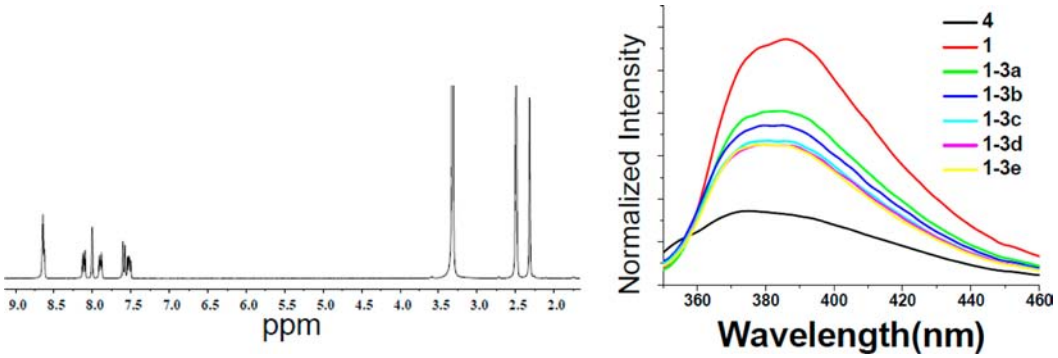

Figure 12. Left: ^{1}H NMR spectra of **1-3e**, and no MeOH or THF guest molecules found in **1-3e**. Right: Solid-state emission spectra of **1**, **1-3a**, **1-3b**, **1-3c**, **1-3d**, **1-3e**, and **4**.

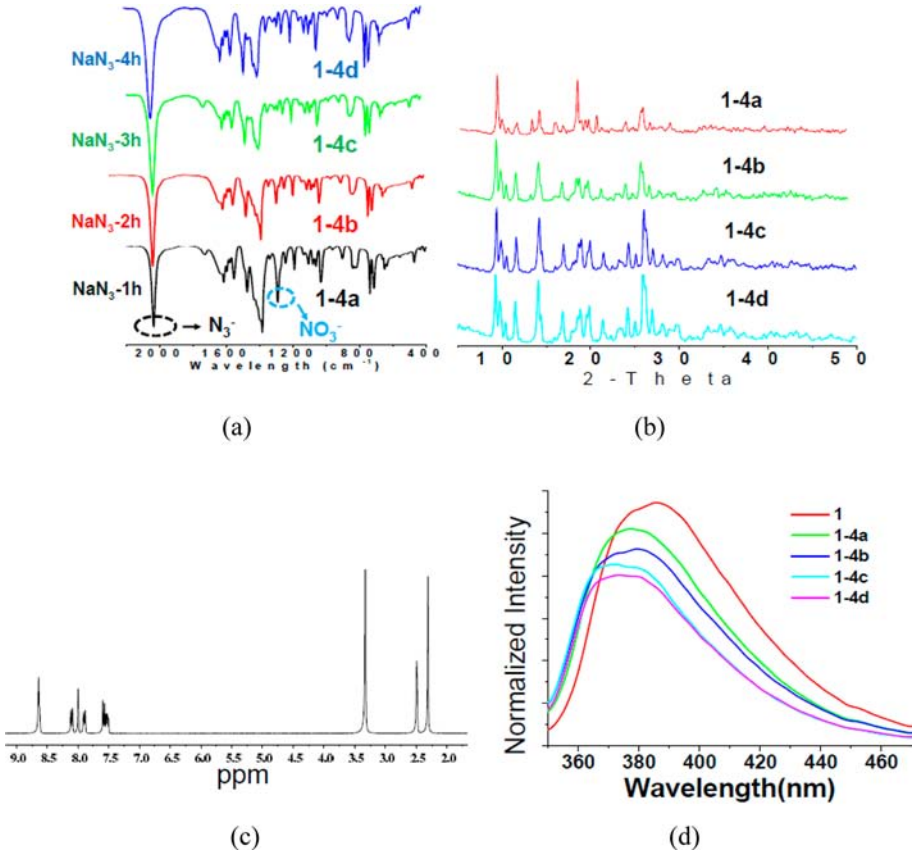

Figure 13. (a) IR spectra of **1** stirred in a MeOH solution of NaN_3 at 1 h (**1-4a**), 2 h (**1-4b**), 3 h (**1-4c**), and 4 h (**1-4d**), respectively. (b) Corresponding XRPD patterns of **1-4a** to **1-4d**. (c) ^{1}H NMR spectrum of **1-4d**. (d) Solid-state spectra of **1**, **1-4a**, **1-4b**, **1-4c**, and **1-4d**.

degrees with suspension time. The XRPD pattern of the ion-exchanged product (**1-1c**) is fully coincident with that of **2** as prepared from $CdCl_2$ and **L**, indicating that the structure of **1** was converted to that of **2** in the solid state by the anion exchange of NO_3^- for Cl^- (from $P2(1)/c$ to $P\bar{1}$). However, the ion-exchanged sample did not diffract the X-ray beams due to the loss of the single crystallinity. To further confirm such a structural transformation is an anion-induced process, a parallel experiment was carried out: When **1** was suspended in MeOH without KCl, XRPD patterns indicated that no structural transformation occurred.

Besides structural transformation, replacement of the nitrate anion with the chloride anion also affects luminescent properties of the Cd-MOFs enormously. As shown in Figure 7, the luminescence of **1** exhibits a broad emission peak at 386 nm (λ_{ex} = 343 nm). The emission of **1-1c**, however, is blue shifted to 373 nm with a second, less intense band present at 357 nm (λ_{ex} = 343 nm), which is identical to that of **2**.

It is similar to Cl^-; Br^- is also able to completely replace the NO_3^- in **1** and, furthermore, induced a solid-to-solid structural transformation in MeOH. Compared to the NO_3^- exchange with Cl^-, the anion-exchange rate of NO_3^- by Br^- finished significantly faster. As indicated by IR spectra, the anion-exchange reaction finished within half an hour (Figure 8). XPS and solid-state emission spectra unambiguously confirm that the Br^- (67.86 eV, Br 2d) anions entered the crystal lattice (Figure 9). In addition, the ion chromatograph (For CdL_2-$Br_2{\cdot}2CH_3OH$, the calculated and observed Br^- amounts are 13.95 and 13.78%, respectively) indicated that the NO_3^- in **1** was quantitatively exchanged with Br^-. XRPD patterns indicate

dx.doi.org/10.1021/ic302716n | Inorg. Chem. 2013, 52, 3225−3235

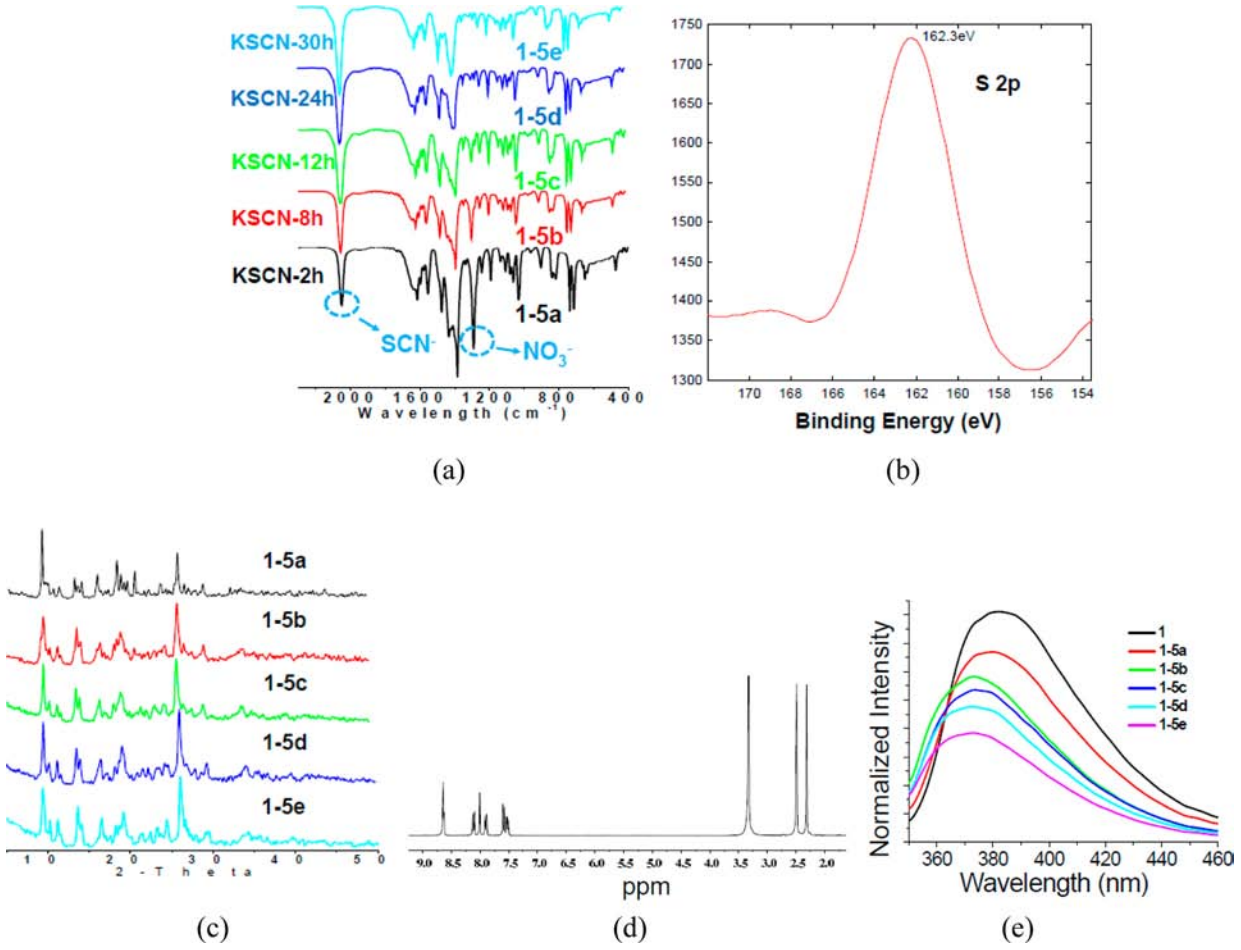

Figure 14. (a) IR spectra of **1** stirred in a MeOH solution of KSCN at 2 h (**1-5a**), 8 h (**1-5b**), 12 h (**1-5c**), 24 h (**1-5d**), and 48 h (**1-5e**), respectively. (b) XPS spectrum of **1-5e**. (c) Corresponding XRPD patterns of **1-5a** to **1-5e**. (d) ^{1}H NMR spectrum of **1-5e**. (e) Solid-state spectra of **1**, **1-4a**, **1-5b**, **1-5c**, **1-5d**, and **1-5e**.

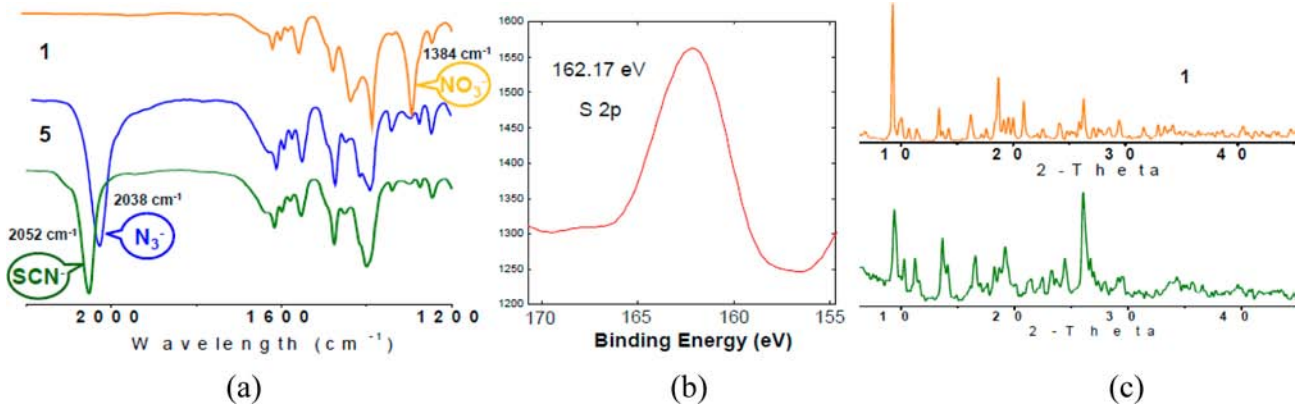

Figure 15. (a) IR spectra of **1** (orange), **5** (blue), and the sample (green) obtained from a mixed MeOH solution containing equimolar SCN^- and N_3^-. (b) XPS spectrum of the sample obtained from a mixed MeOH solution containing equimolar SCN^- and N_3^-. (c) XRPD patterns of **1** (orange) and the sample (green) obtained from a mixed MeOH solution containing equimolar SCN^- and N_3^-.

that the space group of **2** changed from $P2(1)/c$ to $P\bar{1}$ (Figure 8). Again, concomitant with this anion exchange, the solvent guest changed from THF to MeOH, which is well demonstrated by the ^{1}H NMR spectrum (Figure 9) and TGA (Figure 10). Reasonably, **1-2d** and compound **3** exhibit the similar emission property, as indicated in Figure 10.

The above result is significant because anion exchange occurred quantitatively in the solid state and the process accompanied the solid-state structural transformation. Up to date, there have been a handful reports of the light-, heat-, pressure-, or machinery-induced structural transformation in the solid state. However, most of these were observed with the crystals of simple molecules instead of the polymeric coordination frameworks.

Besides Cl^- and Br^-, the NO_3^- anions in **1** can also be completely replaced by I^- in MeOH, but it took a longer time.

dx.doi.org/10.1021/ic302716n | Inorg. Chem. 2013, 52, 3225−3235

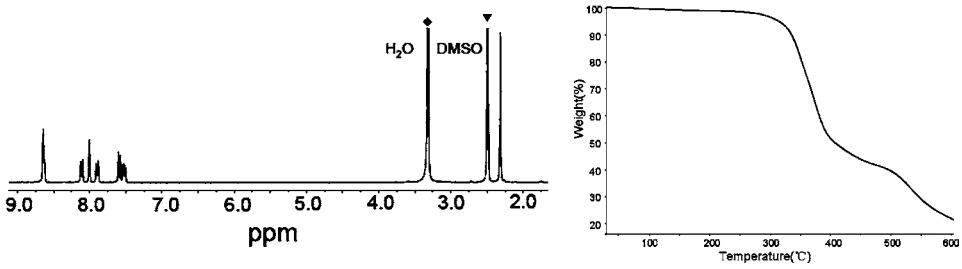

Figure 16. ^{1}H NMR (left) and XPS (right) spectra of the sample obtained from a mixed MeOH solution containing equimolar SCN^- and N_3^-.

The IR spectra monitoring (Figure 11) shows that the anion exchange of NO_3^- with I^- finished within 6 h, which was further confirmed by the XPS spectrum (Figure 11). However, the XRPD monitoring (Figure 11) shows that the replacement of NO_3^- by I^- did not result in a structural transformation. In addition, no solvent guest molecule exchange was found during the ion-exchange, which is confirmed by and ^{1}H NMR spectra (Figure 12) and elemental analysis (Anal. Calcd. for CdL_2I_2: C, 53.15; H, 3.43; N, 9.53. Found: C, 52.02; H, 3.63; N, 9.29). Compared to compound **1**, the solid sample of **1-3e** shows the same emission wavelength, but with a low-energy emission upon photoexcitation at 343 nm at room temperature (Figure 12). In contrast, compound **4** displays a very low-energy emission at around 375 nm (Figure 12). Given that there is a clear red shift (32 nm) on going from **1-3e** to **4**, this could be additional evidence for nonstructural transformation during the anion-exchange process. The low intensity emission of **1-3e** is most likely to have originated from an iodide-to-metal ion charge-transfer transition, based on the strong σ-donating strength of iodide, which is observed in many previous reports.[11]

Besides spherical halide anions Cl^-, Br^-, and I^-, we envisioned if the linear triatomic anions, such as N_3^- and SCN^-, could be used to exchange the trigonal planar NO_3^- in **1**. When the solid **1** was immersed in a MeOH solution of 0.30 M NaN_3 for 4 h, most of the NO_3^- anion of **1** was exchanged with N_3^- in the crystalline state, which was indicated by the disappearance of NO_3^- stretching at 1292 cm^{-1} and the appearance of a new peak at 2035 cm^{-1}, which corresponds to the N_3^- anion. The corresponding XRPD patterns (Figure 13) confirm that the structure of **1** was maintained during the ion-exchange process. Elemental analysis (elemental analysis for **1-4d**: C, 58.21; H, 4.51; N, 17.93) indicates that around 75% of NO_3^- in **1** was exchanged by N_3^-. The ^{1}H NMR spectrum shows that no solvent guest molecules were encapsulated (Figure 13). The emission spectra indicate that the emission band is blue shifted (from 386 nm of **1** to 378 nm of **1-4d**), concomitant with a reduced intensity.

Similarly, the NO_3^- anion of **1** could be mostly exchanged with SCN^- when the crystals of **1** were immersed in the MeOH solution of KSCN (0.30 M) for 30 h, which is well documented by the IR (Figure 14a). The characteristic adsorption band of SCN^- appeared at 2051 nm, and its maximum band intensity is found after 3 h. As shown in Figure 14b, XPS observation of the S 2p (163.2 eV) peak well supported the existence of sulfur in the ion-exchanged product. It is similar to the above cases; no structural transformation occurred during the anion-exchange process, which is verified by the XRPD patterns (Figure 14b). Again, the encapsulated THF molecules were lost during the anion-exchange process in MeOH (Figure 14c). ICP and elemental analysis (elemental analysis for **1-5e**: C, 59.35; H, 3.92; N, 13.04; S, 5.77) indicates that around 94% of NO_3^- of **1** was replaced.

For further confirmation that the above anion exchange is a solid-state process, ^{1}H NMR spectra for the MeOH filtrates were measured. Except for NO_3^- by I^-, no ligand signals in the filtrates were detected in the ^{1}H NMR spectra, so the possibility of the dissolution−reaction−recrystallization process can be definitely excluded (Supporting Information). Notably, all the anion-exchange reactions mentioned above are not reversible. As shown above, the NO_3^- replaced by Cl^- and Br^- anions resulted in the anion-induced new structures that might be more thermodynamically stable than that of **1** and also have different metal−heteroatom bond formation energies (Supporting Information). For SCN^- and N_3^- anions, the anion exchange might reflect the Hofmeister series.[12]

Anion Selectivity Based on 1. Compared to anion exchange, anion selectivity is more attractive and challenging. We[5e,g] and others[4c,5c,13] described some examples of anion separation based on MOFs. As described above, the trigonal planar in **1** can be completely replaced by spherical halide anions Cl^-, Br^-, and I^- and mostly exchanged with linear triatomic SCN^- and N_3^- anions, so we wondered if **1** could be an anion separator to separate these anions with similar geometry. The anion selectivity based on **1** was carried out with only the SCN^-/N_3^- pair because the halide anions are able to cause the structural transformation of **1**.

When the crystals of **1** were soaked in a MeOH solution of equimolar KSCN and NaN_3 (0.03 mol/L) for 30 h, in the IR spectra, only the characteristic band of SCN^- (2052 cm^{-1}) was found, while the characteristic bands of N_3^- (2038 cm^{-1}) and NO_3^- (1292 cm^{-1}), however, were not observed (Figure 15a). The existence of SCN^- was further confirmed by the X-ray photoelectron spectroscopy (Figure 15b). XRPD patterns (Figure 15c) confirm that no structural transformation occurred, and the ^{1}H NMR spectrum and TGA (Figure 16) demonstrate that no solvent molecules were loaded during the selective process. Therefore, the affinity based on **1** obeys the following order: $SCN^- > N_3^-$. Elemental analysis (Found: C, 59.52; H, 3.95; N, 13.10; S, 5.75) indicates that about 93.5% of NO_3^- was replaced by SCN^-.

CONCLUSIONS

In summary, we have described a series of interesting Cd(II) coordination polymers that are constructed from a new oxadiazole-bridged ligand **L** and CdX_2 (X = NO_3^-, Cl^-, Br^-, I^-, N_3^-, and SCN^-). The NO_3^- anion of the solid $CdL_2(NO_3)_2{\cdot}2THF$ (**1**) is able to be quantitatively exchanged with Cl^-, Br^-, I^-, SCN^-, and N_3^- in the solid state, when the crystals of **1** were immersed in MeOH solutions of the corresponding anions. For Cl^- and Br^-, the anion exchange resulted in a anion-induced structural transformation to form

dx.doi.org/10.1021/ic302716n | Inorg. Chem. 2013, 52, 3225−3235

the structures of **2** and **3**, respectively. In addition, the Cd(II) structure herein exhibits the anion-responsive photoluminescence, which could be a useful method to monitor the anion-exchange process. Notably, compound **1** can recognize and completely separate SCN^-/N_3^- with similar geometry.

■ ASSOCIATED CONTENT

Supporting Information

Crystallographic data in CIF format, further details for compounds **3**–**6** (including ^1H NMR, TGA, coordination patterns, and XRPD), ^1H NMR spectra for MeOH filtrates, and calculated Cd(II)-heteroatom formation energies. This material is available free of charge via the Internet at http://pubs.acs.org.

■ AUTHOR INFORMATION

Corresponding Author

*E-mail: yubindong@sdnu.edu.cn.

Notes

The authors declare no competing financial interest.

■ ACKNOWLEDGMENTS

We are grateful for financial support from the NSFC (Grant Nos. 91027003, 21072118, 21271120, and 21101100), the 973 Program (Grant Nos. 2013CB933800, 2012CB821705), "PCSIRT", and the Shangdong Natural Science Foundation (Grant No. BS2012CL035).

■ REFERENCES

(1) (a) Deng, H. X.; Doonan, C. J.; Furukawa, H.; Ferreira, R. B.; Towne, J.; Knobler, C. B.; Wang, B.; Yaghi, O. M. *Science* **2010**, *327*, 846. (b) Cohen, S. M. *Chem. Rev.* **2012**, *112*, 970. (c) Li, J.-R.; Sculley, J.; Zhou, H.-C. *Chem. Rev.* **2012**, *112*, 970. (d) Zhang, J.-P.; Zhang, Y,-B.; Lin, J.-B.; Chen, X.-M. *Chem. Rev.* **2012**, *112*, 1001. (e) Wu, H.; Gong, Q.; Olson, D. H.; Li, J. *Chem. Rev.* **2012**, *112*, 836. (f) Wang, C.; Zhang, T.; Lin, W. *Chem. Rev.* **2012**, *112*, 1084. (g) Horcajada, P.; Gref, R.; Baati, T.; Allan, P. K.; Maurin, G.; Couvreur, P.; Férey, G.; Morris, R. E.; Serre, C. *Chem. Rev.* **2012**, *112*, 1232. (h) Yoon, M.; Srirambalaji, R.; Kim, K. *Chem. Rev.* **2012**, *112*, 1196. (i) Suh, M. P.; Park, H. J.; Park, H. J.; Prasad, T. K.; Lim, D.-W. *Chem. Rev.* **2012**, *112*, 782. (j) Kreno, L. E.; Leong, K.; Farha, O. K.; Allendorf, M.; Van Duyne, R. P.; Hupp, J. T. *Chem. Rev.* **2012**, *112*, 1105. (k) Sumida, K.; Rogow, D. L.; Mason, J. A.; McDonald, T. M.; Bloch, E. D.; Herm, Z. R.; Bae, T.-H.; Long, J. R. *Chem. Rev.* **2012**, *112*, 724.

(2) (a) Gale, P. A. *Coord. Chem. Rev.* **2003**, *240*, 191. (b) Gale, P. A.; Quesada, R. *Coord. Chem. Rev.* **2006**, *250*, 3219. (c) Filby, M. H.; Steed, J. W. *Coord. Chem. Rev.* **2006**, *250*, 3200. (d) Vilar, R. *Angew. Chem., Int. Ed.* **2003**, *42*, 1460. (e) Custelcean, R.; Moyer, B. A. *Eur. J. Inorg. Chem.* **2007**, 1321.

(3) Gimeno, N.; Vilar, R. *Coord. Chem. Rev.* **2006**, *250*, 3161.

(4) (a) Min, K. S.; Suh, M. P. *J. Am. Chem. Soc.* **2000**, *122*, 6834. (b) Jung, O.-S.; Kim, Y. J.; Lee, Y.-A.; Park, J. K.; Chae, H. K. *J. Am. Chem. Soc.* **2000**, *122*, 9921. (c) Halper, S. R.; Do, L.; Stork, J. R.; Cohen, S. M. *J. Am. Chem. Soc.* **2006**, *128*, 15255. (d) Schottel, B. L.; Chifotides, H. T.; Shatruk, M.; Chouai, A.; Pérez, L. M.; Bacsa, J.; Dunbar, K. R. *J. Am. Chem. Soc.* **2006**, *128*, 5895. (e) Biswas, C.; Mukherjee, P.; Drew, M. G. B.; Gómez-García, C. J.; Clemente-Juan, J. M.; Ghosh, A. *Inorg. Chem.* **2007**, *46*, 10771. (f) Halper, S. R.; Do, L.; Stork, J. R.; Cohen, S. M. *J. Am. Chem. Soc.* **2006**, *128*, 15255.

(5) (a) Cui, Y.; Yue, Y.; Qian, G.; Chen, B. *Chem. Rev.* **2012**, *112*, 1126. (b) Caltagirone, C.; Gale, P. A. *Chem. Soc. Rev.* **2009**, *38*, 520. (c) Fei, H.; Bresler, M. R.; Oliver, S. R. J. *J. Am. Chem. Soc.* **2011**, *133*, 11110. (d) Chen, B.; Wang, L.; Zapata, F.; Qian, G.; Lobkovsky, E. B. *J. Am. Chem. Soc.* **2008**, *130*, 6718. (e) Wong, K.-L.; Law, G. L.; Yang, Y.-Y.; Wong, W.-T. *Adv. Mater.* **2006**, *18*, 1051. (f) Ma, J.-P.; Yang, Y.; Dong, Y.-B. *Chem. Commun.* **2012**, *48*, 2917. (g) Fang, C.; Liu, Q.-K.; Ma, J.-P.; Dong, Y.-B. *Inorg. Chem.* **2012**, *51*, 3923.

(6) (a) Sheldrick, G. M. *SHELXTL*, Version 5.12; Bruker Analytical X-ray Systems, Inc.: Madison, WI, 1997. (b) Spek, A. L. *PLATON: A Multipurpose Crystallographic Tool*; University of Utrecht: Utrecht, the Netherlands, 1998.

(7) Zaman, M. B.; Smith, M. D.; zur Loye, H.-C. *Chem. Mater.* **2001**, *13*, 3534.

(8) Dong, Y.-B.; Smith, M. D.; Layland, R. C.; zur Loye, H.-C. *Chem. Mater.* **2000**, *12*, 1159.

(9) (a) Michaelides, A.; Skoulika, S. *Crystal Growth Des.* **2009**, *9*, 2039. (b) Nagarathinam, M.; Chanthapally, A.; Lapidus, S. H.; Stephens, P. W.; Vittal, J. J. *Chem. Commun.* **2012**, *48*, 2585. (c) Safarifard, V.; Morsali, A. *CrystEngComm* **2011**, *13*, 4817.

(10) (a) Addison, C. C.; Amos, D. W.; Sutton, D. *J. Chem. Soc. A* **1967**, 808. (b) Carnall, W.; Siegel, S.; Ferrano, J.; Tani, B.; Gebert, E. *Inorg. Chem.* **1973**, *12*, 560. (c) Nakamoto, K. *Infrared and Raman Spectra of Inorganic and Coordination Compounds*, 5th ed.; John Wiley: New York, 1997.

(11) Liu, Q.-K.; Ma, J.-P.; Dong, Y.-B. *Chem. Commun.* **2011**, *47*, 7185.

(12) (a) Hofmeister, F. *Arch. Exp. Pathol. Pharmakol.* **1888**, *24*, 247. (b) Kunz, W.; Henle, J.; Ninham, B. W. *Curr. Opin. Colloid Interface Sci.* **2004**, *9*, 19.

(13) Custelcean, R.; Haverlock, T. J.; Moyer, B. A. *Inorg. Chem.* **2006**, *45*, 6446.